REPORT DOCUMENTATION PAGE

Form Approved OMB NO. 0704-0188

1. REPORT DATE (DD-MM-YYYY)	2. REPORT TYPE	3. DATES COVERED (From - To)
11-01-2016	Final Report	1-Aug-2013 - 31-Jul-2014

4. TITLE AND SUBTITLE
Final Report: Integrated Real-Time Control and Imaging System for Microbiorobotics and Nanobiostructures

5a. CONTRACT NUMBER
W911NF-13-1-0304

5b. GRANT NUMBER

5c. PROGRAM ELEMENT NUMBER
611103

6. AUTHORS
MINJUN KIM

5d. PROJECT NUMBER

5e. TASK NUMBER

5f. WORK UNIT NUMBER

7. PERFORMING ORGANIZATION NAMES AND ADDRESSES
Drexel University
Office of Research
3201 Arch Street, Suite 100
Philadelphia, PA 19104 -2875

8. PERFORMING ORGANIZATION REPORT NUMBER

9. SPONSORING/MONITORING AGENCY NAME(S) AND ADDRESS (ES)
U.S. Army Research Office
P.O. Box 12211
Research Triangle Park, NC 27709-2211

10. SPONSOR/MONITOR'S ACRONYM(S)
ARO

11. SPONSOR/MONITOR'S REPORT NUMBER(S)
63548-NS-RIP.1

12. DISTRIBUTION AVAILIBILITY STATEMENT
Approved for Public Release; Distribution Unlimited

13. SUPPLEMENTARY NOTES
The views, opinions and/or findings contained in this report are those of the author(s) and should not contrued as an official Department of the Army position, policy or decision, unless so designated by other documentation.

14. ABSTRACT
This project is to develop a novel integrated system module with digital light processing (DLP) and total internal reflection fluorescence microscopy (TIRFM) for scientific research and education in microbiorobotics for manipulation, and sensing, and biologically inspired metamaterials for nanoelectronics. The multi-functional capacity provided by an integrated DLP-TIRFM system will enable researchers and students to perform material imaging, manipulation, and property measurements with optical, electrical, mechanical, and thermal stimulation. Specific research projects include: (1) feedback control of multiple bacteria-powered microrobots using DLP

15. SUBJECT TERMS
Digital Light Processing, Total Internal Reflection Fluorescence, Optical Microscopy

16. SECURITY CLASSIFICATION OF:			17. LIMITATION OF ABSTRACT	15. NUMBER OF PAGES	19a. NAME OF RESPONSIBLE PERSON
a. REPORT	b. ABSTRACT	c. THIS PAGE			Minjun Kim
UU	UU	UU	UU		19b. TELEPHONE NUMBER 215-895-2295

Report Title

Final Report: Integrated Real-Time Control and Imaging System for Microbiorobotics and Nanobiostructures

ABSTRACT

This project is to develop a novel integrated system module with digital light processing (DLP) and total internal reflection fluorescence microscopy (TIRFM) for scientific research and education in microbiorobotics for manipulation, and sensing, and biologically inspired metamaterials for nanoelectronics. The multi-functional capacity provided by an integrated DLP-TIRFM system will enable researchers and students to perform material imaging, manipulation, and property measurements with optical, electrical, mechanical, and thermal stimulation. Specific research projects include: (1) feedback control of multiple bacteria-powered microrobots using DLP control modality, (2) investigation and visualization of the hydrodynamic flagella coordination in the lubrication layer of bacteria, and (3) advanced imaging and characterization of flagellar polymorphic transitions of flagella forests and flagella-templated nanotubes. Demonstration of phototactic/thermotactic control capabilities on microorganism-based robotics will have great impact on control systems theory and engineering. In addition, characterizing and understanding biological and synthetic micro/nanoscale structures is crucial in the continued push for micro/nanotechnologies while synthetic materials would combine biological properties with the ease of handling inorganic molecules.

Enter List of papers submitted or published that acknowledge ARO support from the start of the project to the date of this printing. List the papers, including journal references, in the following categories:

(a) Papers published in peer-reviewed journals (N/A for none)

Received Paper

TOTAL:

Number of Papers published in peer-reviewed journals:

(b) Papers published in non-peer-reviewed journals (N/A for none)

Received Paper

TOTAL:

Number of Papers published in non peer-reviewed journals:

(c) Presentations

Number of Presentations: 0.00

Non Peer-Reviewed Conference Proceeding publications (other than abstracts):

Received Paper

TOTAL:

Number of Non Peer-Reviewed Conference Proceeding publications (other than abstracts):

Peer-Reviewed Conference Proceeding publications (other than abstracts):

Received Paper

TOTAL:

Number of Peer-Reviewed Conference Proceeding publications (other than abstracts):

(d) Manuscripts

Received Paper

TOTAL:

Number of Manuscripts:

Books

Received Book

TOTAL:

Received Book Chapter

TOTAL:

Patents Submitted

Patents Awarded

Awards

Graduate Students

NAME	PERCENT_SUPPORTED	Discipline
PAUL KIM	1.00	
FTE Equivalent:	**1.00**	
Total Number:	**1**	

Names of Post Doctorates

NAME	PERCENT_SUPPORTED
FTE Equivalent:	
Total Number:	

Names of Faculty Supported

NAME	PERCENT_SUPPORTED	National Academy Member
MINJUN KIM	1.00	
FTE Equivalent:	**1.00**	
Total Number:	**1**	

Names of Under Graduate students supported

NAME	PERCENT_SUPPORTED
FTE Equivalent:	
Total Number:	

Student Metrics

This section only applies to graduating undergraduates supported by this agreement in this reporting period

The number of undergraduates funded by this agreement who graduated during this period: 0.00

The number of undergraduates funded by this agreement who graduated during this period with a degree in science, mathematics, engineering, or technology fields:..... 0.00

The number of undergraduates funded by your agreement who graduated during this period and will continue to pursue a graduate or Ph.D. degree in science, mathematics, engineering, or technology fields:..... 0.00

Number of graduating undergraduates who achieved a 3.5 GPA to 4.0 (4.0 max scale):..... 0.00

Number of graduating undergraduates funded by a DoD funded Center of Excellence grant for Education, Research and Engineering:..... 0.00

The number of undergraduates funded by your agreement who graduated during this period and intend to work for the Department of Defense 0.00

The number of undergraduates funded by your agreement who graduated during this period and will receive scholarships or fellowships for further studies in science, mathematics, engineering or technology fields: 0.00

Names of Personnel receiving masters degrees

NAME
Total Number:

Names of personnel receiving PHDs

NAME
Total Number:

Names of other research staff

NAME	PERCENT_SUPPORTED
FTE Equivalent:	
Total Number:	

Sub Contractors (DD882)

Inventions (DD882)

Scientific Progress

DURIP Equipment Summary
Several major components have been acquired and outlined below.
Nikon Ti-Eclipse Microscope with Andor iXon3 Camera
Total internal reflection fluorescence (TIRF) microscope is able to capture and image with great detail and offers superior visual study of samples. Most components on the microscope are motorized and controlled through the software suite. The microscope has come equipped with an Andor iXon3 camera. The main highlight of this equipment is its ability to capture images with a high EM gain.
Digital Light Innovations DLi 4120 DLP Bundle
The DLi 4120 is a DLP kit with a control board and ALP 4.1 basic controller suite. The digital micromirror device is the highest resolution 16:9 aspect ratio system. This DMD has a high transmission with visible light. Patterns can be generated on the DMD using GUI commands as well as interfacing the API any popular coding language. For this system, a 980nm laser diode was purchased for use in localized heating on a microscope sample.

See the attachment

Technology Transfer

N/A

DURIP Equipment Summary

1. INTRODUCTION

This equipment summary outlines the development and research outcomes of the combined system composed of digital light processing (DLP) integrated with high resolution fluorescence microscopy and electromagnetic manipulators. The integrated system enabled the PI's group to perform property measurements of stimuli-responsive biotic and abotic nano/microstructures in microfluidic environments, as well as swarm control of hybrid biotic-abiotic microbiorobots for manipulation and sensing. The impact of the purchased tools on the supported Amy Research Office (ARO) Young Investigator Program and the ARO Complex Dynamics and Systems Program are outlined. In addition, we report on the impact of these assets in our on-going educational and collaborative programs.

2. SYSTEM OVERVIEW

The acquired system components, shown in Figure 1, consisted of the following: (1) digital micromirror device (DMD) and controller, (2) an inverted epifluorescence microscope with a flat top motorized stage, TIRF arm, and EMCCD camera, and (3) two electromagnetic manipulators. The DLP system purchased was a DLi 4120 is a DLP kit with accompanying control board and ALP 4.1 basic controller suite. The digital micromirror device is currently the highest commercially available resolution, and has a 16:9 aspect ratio. This DMD has high transmission with visible light. Patterns can be generated on the DMD using GUI commands as well as interfacing the API with any popular coding language. For this system, a 980nm laser diode was purchased for use in localized heating on a microscope sample. The microscope acquired was a Nikon Ti-Eclipse inverted microscope equipped with an LED epi-fluorescence illuminator, dichroic mirror filter set, TIRF arm, and a PRIOR Scientific H117 programmable motorized stepper stage with a minimum step size of 0.01 microns. In addition to the standard 10× – 100× objectives, one Nikon 100× oil immersion TIRF objective (1.25 NA) was obtained for TIRF imaging. For fluorescence image capture, an Andor iXon3 897 back-illuminated EMCCD camera was also purchased. The two electromagnetic manipulators used were (1) a custom built approximate Helmholtz Coil system that consisted of a 3D-printed holder that housed six epoxy-wound copper coils, and (2) a galvanotatic system that consisted of a polydimethylsiloxane-glass chamber with imbedded platinum wires and filled with an electrolytic solution.

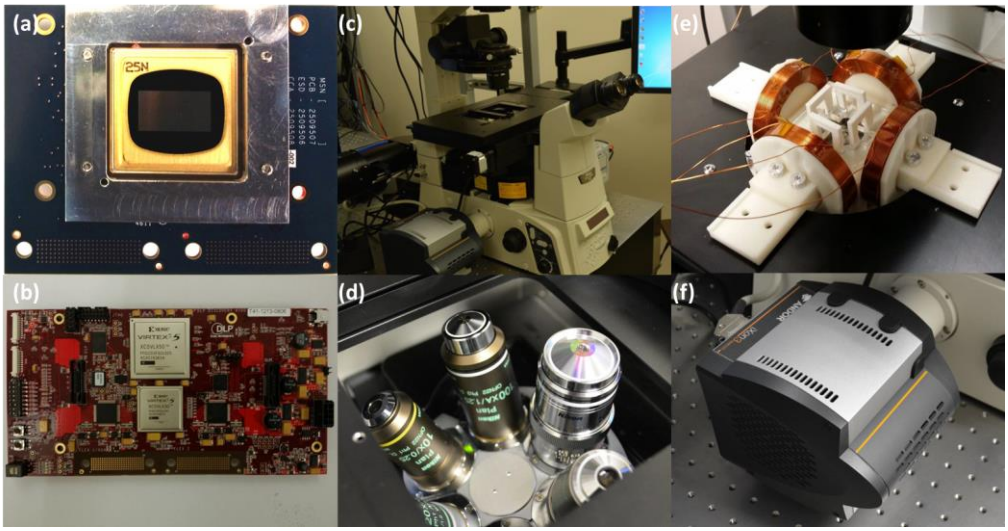

Figure 1: *Equipment acquired through the DURIP (a) Texas Instruments Discovery D4100 micromirror array (b) DLP control board (c) Nikon Ti Eclipse inverted epi-fluorescence microscope with TIRF Arm (d) Motorized turrets and objectives including 100× TIRF objective (e) Electromagnetic manipulation system (f) Andor iXon3 897 back-illuminated EMCCD.*

2.1 System Set-Up and Integration

In order to facilitate experiments the acquired equipment needed to be set-up, or in some cases modified, to enable integration with other system components. For integration of the DLP system with the microscope we built custom acrylic block holders for both the DMD and its control board (Figure 2(b)). The housed DMD was mounted on a three-axis positioner and oriented at an angle that allowed laser light to reflect into the inverted microscope. To control the tilt angle of the DMD's micromirrors the control board was interfaced with a computer through a PCI-E connection. There was no special set-up needed for the Nikon microscope, however the base plate of the flat top motorized stage had to be modified to fit our approximate Helmholtz Coil system. With the stage modification both the coil system and galvanotatic system were able to fit within the microscope stage with sufficient travel distance (Figure 2(d)).

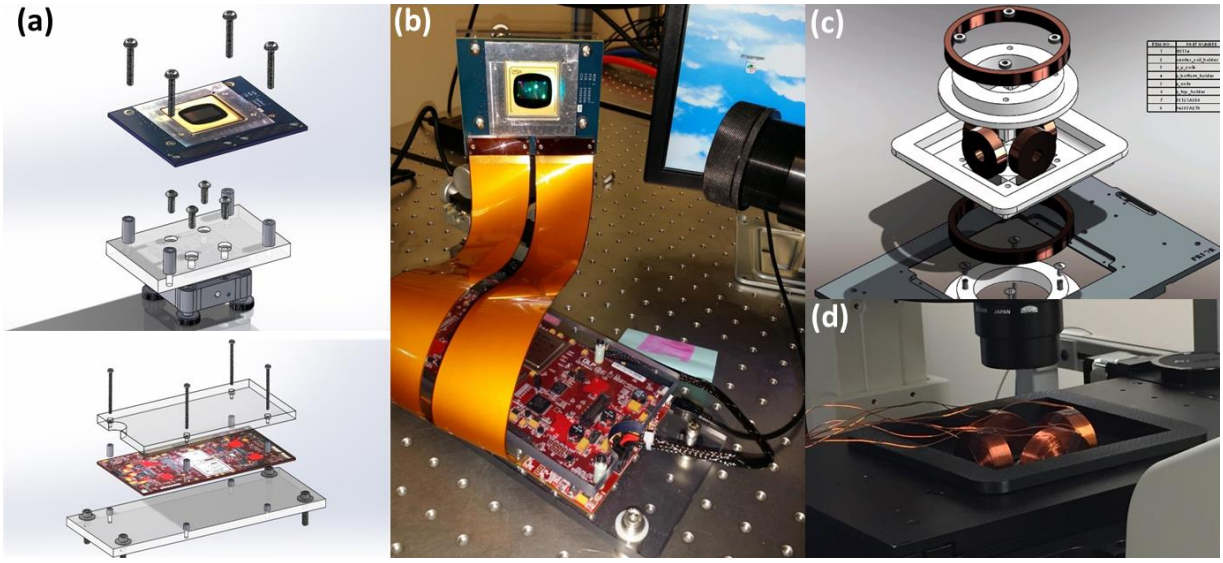

Figure 2: *Set-Up and integration of DLP/high resolution fluorescence microscopy and electromagnetic manipulators (a) 3D schematic of DMD holder (top) and controller (bottom) (b) Final DLP system set-up (c) 3D schematic of approximate Helmholtz Coil system (f) Final 3D printed coil system integrated within the PRIOR Scientific H117 programmable motorized stepper stage and Nikon inverted microscope.*

3. EQUIPMENT IMPACT ON ARMY RESEARCH OFFICE-FUNDED RESEARCH

The acquired equipment was essential to achieve the activities outlined in our ARO funded programs. Acquisition and integration of the DLP system with high resolution microscopy has enabled vision-based control of microbiorobots, as well as imaging and characterization of nano/microstructures in response to structural, mechanical, optical, and thermal stimuli. With the integrated system we have been able to further develop ongoing microrobotics research programs to achieve microscale task with improved control and multi robot control, in which microrobots have been made to perform autonomous tasks in response to external global control signals. We envision that these control and microscale tasks will enable our microrobots to be used for unique biotechnical applications for drug delivery, cell therapy, improving recovery time, treatment methods, and survivability for soldiers on the field.

3.1 Microbiorobotics for Manipulation and Sensing

The objective of this research project was to develop a platform that integrates microorganisms with enhanced motility and signaling behavior into a microscale sensing and robotics system. The integrated high resolution microscopy system allowed the PI's group to acquire an in-depth understanding of the

fundamental scientific principles that govern the control of bacterial propulsion systems, as well as demonstration of the enabling technologies necessary to accomplish the feedback swarm control of bacteria-powered microstructures for use in micro-assembly and microbiorobotics. The acquired system was applicable in studying microscale assembly platforms and biosensors that required autonomous coordination of bacteria.

A. Control of Bacteria-Powered Microrobots Using Static Obstacle Avoidance Algorithm

A bacteria-powered microrobot (BPM) is a hybrid robotic system consisting of an SU-8 microstructure with active surfaces composed of a monolayer of unpattered swarming bacteria, in which massive arrays of biomolecular flagellar motors work cooperatively. The equipment obtained for this project enabled us to successfully develop an autonomous navigation algorithm for BPM obstacle avoidance. Moreover, we have demonstrated obstacle avoidance in cluttered environments modifying different parameters in our algorithm [1].

Briefly, BPMs were fabricated by first using conventional photolithography with SU-8 negative photoresist to pattern 20 µm thick microstructures on glass slides coated with a water-soluble sacrificial dextran layer. After exposure and development the 32 µm × 30 µm rectangular SU-8 patterns were blotted on the leading edge of a swarming colony of *S. marcescens* grown on an agar plate. BPMs were placed in an experimental chamber composed of polydimethylsiloxane (PDMS) that contained obstacles which were fabricated on the underling glass substrate using traditional soft lithography. The chamber was filled with a motility buffer and 0.05% polyethyleneglycol (PEG). Two pairs of platinum wires were fixed in parallel position with respect to horizontal direction and vertical direction generation of DC electric fields through agar salt bridges: Steinberg's solution (0.7mM KCl, 0.8mM $MgSO_4 \cdot 7H_2O$, 60mM NaCl, 0.3mM $CaNO_3 \cdot 4H_2O$). The central portion of the workspace in the chamber is visualized by a camera. General image processing traced the position of the BPM. The localization of the BPM and the environment information in the image were used in our algorithm. Through our strategy, the determined control input from a computer was applied to an analog output board (NI DAQ SCB68) that was connected to two power supplies (Ametek XTR 100-8.5). Fig. 7 shows both paths of the experimental result (red crosses) and the simulation result (blue circles). Using the obstacle avoidance algorithm, the BPM navigated a field of two obstacles without collision with a ~40° angle of direction towards to the the predetermined goal. Our approach defined an objective function in order to choose the optimal velocity from the admissible velocity space at consecutive intervals. The objective function includes *heading*, *movement*, *clearance*, and *control* functions to reflect the aforementioned constraints. The optimal velocity has a maximum cost in the objective function and can be varied depending on the desired weighting for each function. Through several experiments, our proposed method succeeded in translating the BPM to its goal position while avoiding static obstacles. In terms of the control input, our algorithm steadily maintained the maximum magnitude of input, which was 20V in our system. The experiments demonstrated the

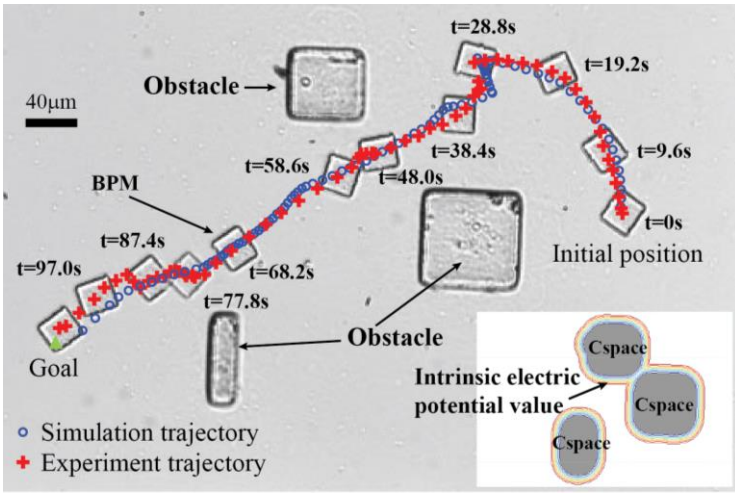

Figure 3: *Experimental implementation of static obstacle avoidance algorithm using electric field controlled Bacteria-Powered Microrobots (BPMs) [1].*

proposed algorithm and proved that our obstacle avoidance method has the potential to control microrobots using electric fields.

B. Visualizing Hydrodynamic Coherence Induced by Bacterial Carpets

The propulsive force of the BPMs is generated by the bacterial carpet which is able to give the microstructure motility. In our previous investigations we demonstrated motion control of these bacteria powered microbiorobots, however without any external stimuli, BPMs display natural rotational and translational movements on their own (Figure 4(b)). This BPM self-actuation is due to the coordination of flagella. Using high resolution microscopy equipment we investigated the flow fields generated by bacterial carpets, and compared this flow to the flow fields observed in the bulk fluid at a series of locations above the bacterial carpet [2]. Microscale particle image velocimetry (micro PIV) experiments were conducted, in which we characterized the flow fields generated from the bacterial carpets of BPMs in an effort to understand their propulsive flow, as well as the resulting pattern

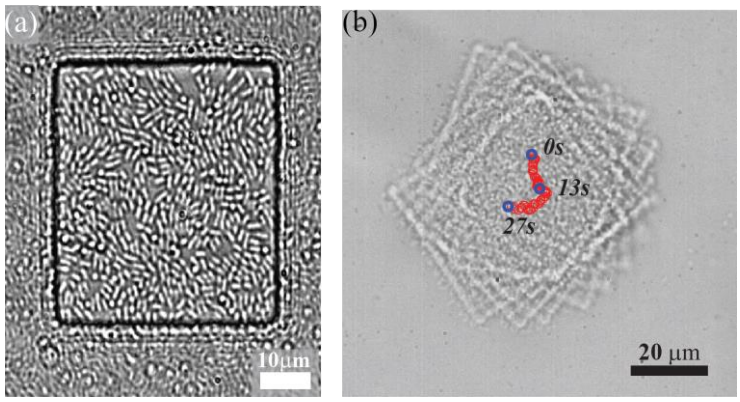

Figure 4: *Bacterial carpet on static structure and self-actuated MBR. (a) Bacterial carpet attached on the structure Fig. 1(b). (b) Self-actuation of a MBR resulted from flagellar motion of the attached bacteria [2].*

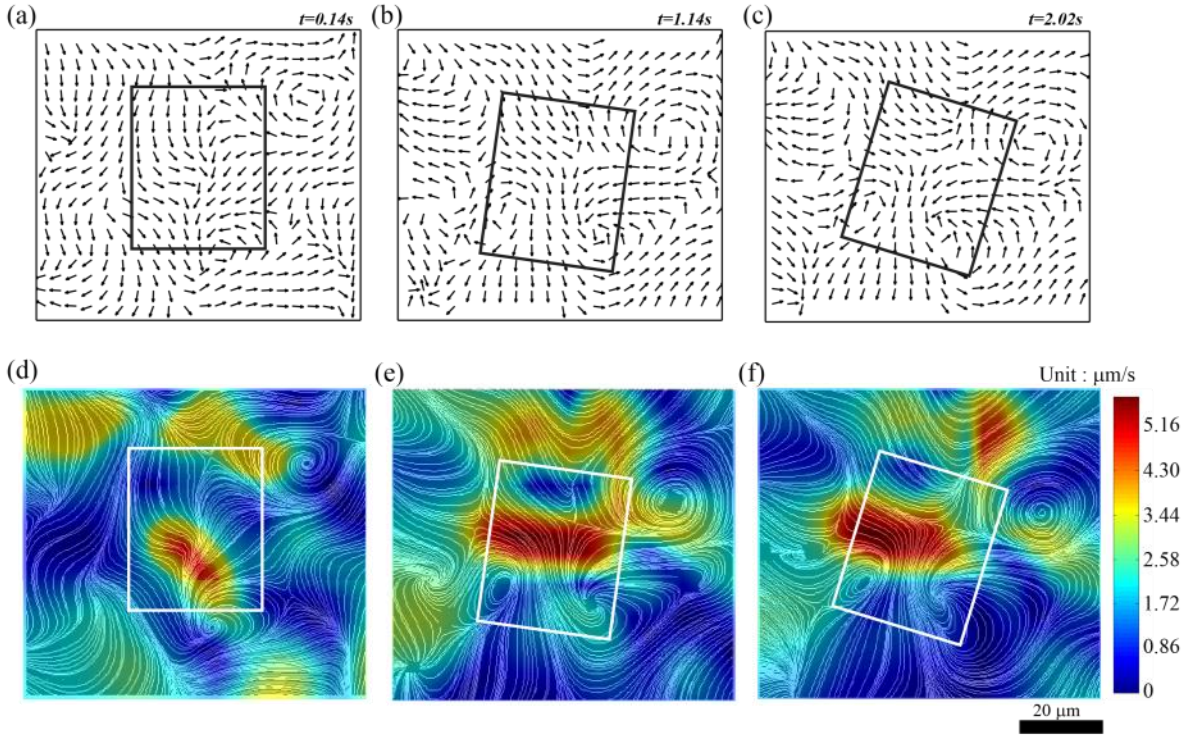

Figure 5: *Velocity flow fields on the moving structure BPM. (a) Velocity flow by micro PIV result data with same scale arrows on the region of the structure at 0.14s. (b) Velocity flow by micro PIV result data with same scale arrows on the region of the structure at 1.14s. (c) Velocity flow by micro PIV result data with same scale arrows on the region of the structure at 2.02s. (d) Streamline and microvortices at 0.14s. (e) Streamline and microvortices at 1.14s. (f) Streamline and microvortices at 2.02s [2].*

of flagella driven self-actuated motion. Comparing the velocities between the bacterial carpets on fixed and untethered BPMs, it was found that flow velocities near the surface of the microstructure were strongest, and at distances far above the surface flow velocities were much smaller. Analyzing flow field streamlines we observed the generation and dissipation of microvortices that rotated either clockwise or counterclockwise. The fluctuation of the ensemble average velocities in these experiments, shown in Figure 5, can be explained by the random switching of flagellar motion on individual bacteria. The independent flagellar rotation change creates peaks and transient oscillations in the flow and the instantaneous strong velocity flow might result from strong hydrodynamic interactions between flagella. This micro PIV analysis provides insights into the flagellar hydrodynamics of bacterial carpets and enhances understanding of the effects of flagella driven boundary flows.

3.2 Collective Response in Flagellar Forests

The flagellar forest is a sensing device that utilizes the natural properties and sensing capabilities of the flagella, thus, it is a new class of sensor used for the detection of various stimuli including electrical, thermal, optical, and chemical. It consists of arrays of flagella attached to magnetic beads that are fixed at patterns on a substrate in a manner where the flagella filaments are tethered at one end. To achieve this, flagellar filaments were first functionalized at one end through biotinylation of flagella seeds followed by polymerization using non-functionalized flagellin. Sequentially, magnetic beads with streptavidin coating are introduced and conjoin with the functionalized flagella to create flagellated magnetic beads. Then, iron oxide is mixed with SU-8 and is photolithographically patterned on a silicon substrate follow by another layer of patterned SU-8, creating a well structure. Finally, flagellated beads are introduced onto the patterned substrate to create a flagellar forest; magnetic beads are securely fixed in the wells by magnetic force.

A. Micro PIV measurements of flows induced by rotating microparticles near a boundary

Before studying the dynamics of the flagellar forest, we first investigated the resultant hydrodynamics of spherical microparticles (with no flagella) rotating near a boundary. In these experiments we used a colloidal solution of deionized water containing carboxylated magnetic microparticles (4 and 8μm in diameter) and 200 nm fluorescent seeding particles that were sealed in borosilicate glass capillaries (inner dimensions 2.00 x 0.05 mm). Images (taken at 500 frames per second) of seeding particles being displaced by the flows induced by rotating microparticles were used to obtain flow field information. Experiments were conducted using the approximate Helmholtz-coil system that was integrated with the high resolution fluorescence imaging system. Filled capillaries were placed in the center of coil system, where a uniform magnetic field of ~15 mT was generated. Magnetic field rotational frequency and orientation (clockwise/counterclockwise) was controlled via a custom LABVIEW program as previously reported [3]. To create a rotational field in the *xy*-plane coil pairs were set to generate sinusoidal signals that were out of phase by 90^{o}. Captured image series were analyzed with commercial PIV software (DaVis 8.0) and time-averaged velocity vector flow fields were generated.

Analysis of flows induced by isolated microparticles showed an exponential flow field decay as the radial distance from the microparticles surface, which is in good agreement with theory and numerical simulation. To obtain insight into three-dimensional flows around isolated particles, two-dimensional flows were obtained at a series of heights (Figure 6). It was observed that measured flow fields below the equatorial plane were significantly smaller than those mirrored on the opposite side of the equator. This result can be attributed to the neighboring boundary which breaks the axial symmetry of the rotational flow field, which is apparent due to strong viscous effects that are a function of the low rotational Reynolds number and the small microparticle-wall gap width. In addition to investigating the flow fields

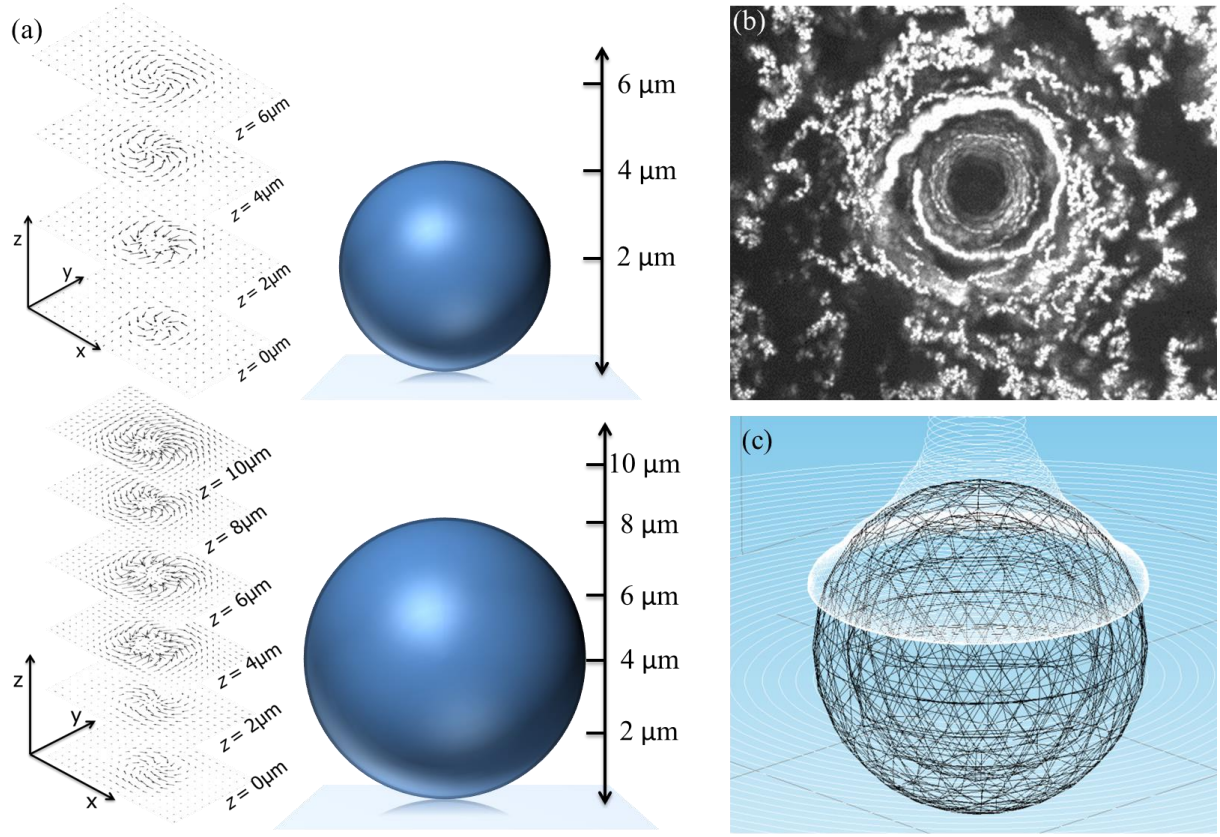

Figure 6: *(a) Characteristic vector flow fields observed at various cross-sections for 4 μm (top) and 8 μm (bottom) diameter microparticles rotating synchronously at 10 Hz. (b) Qualitative flow visualization of stead-state streamlines formed by digital averaging 100 sequential images acquired at 100 Hz. (c) Side view of the streamlines obtained from finite element simulation of 8 μm bead rotating near a boundary.*

generated by isolated microparticles, velocity profiles of two neighboring rotating particles were also analyzed. We found that when two or more microparticles are actuated at low rotational frequencies and have relatively large inter-particle spacing, strong viscous forces limit hydrodynamic interactions between generated flows. However, as the separation distance between active rotors decreases, flow felids begin to interact, leading to hydrodynamic coupling of flows, until individual micro-vortices are indistinguishable and completely merge. From these results it appears that geometric differences between a dimer, i.e. two joined particles, and a single particle with twice the diameter do not significantly contribute to the overall flow, and that the generated flows of a dimer can be closely approximated by the flow of a single larger particle. This investigation will aid in distinguishing between the flows generated by rotating flagella and those generated from rotating spherical particles.

B. Characterization of Individual Flagella in Various Fluidic Environments

Bacterial flagella are self-assembled spiral nanostructures, approximately 20 nm in diameter and 10 micrometers long. As mechanical devices, flagella have extraordinary properties. In response to different environmental stimuli flagella undergo polymorphic transformations, changing their helical handedness and pitch [4]. This transformation is caused by minute (sub-nanometer) realignment in each of the thousands of molecular monomers (flagellin) that form longitudinal rows along the length of the entire flagellar filament. The collective motion of these changes combines to generate changes in length (i.e. strain) by factors as large as three. While these shape changes have been reported, little has been done to extensively study and understand the polymorphic transformation for flagellar filaments, especially the

actual transformation process as well as the transformation timescale. To properly utilize the flagellar forest as a sensor, we investigated the characteristics of polymorphic transitions in individual flagella. The acquired high resolution microscopy equipment was essential to accomplish this task.

Due to their small size bacterial flagella require special preparation and/or imaging equipment for visualization. For imaging, repolymerized flagella were fluorescently tagged with cy3 dye. Because dyed flagella easily photo-bleach and generate blurred images, a relatively weak LED light source was used in conjunction with high electromagnetic gain using the Andor EMCCD camera. Using this method we obtained images of flagella undergoing polymorphic transformations in response to different environmental stimuli (Figure 7). This precise knowledge of polymorphic dynamics through careful characterization of individual flagellar filaments shed light on this biological phenomenon while also bring the potential to fully utilize the natural properties of bacterial flagella in the flagellar forest for application in engineering systems.

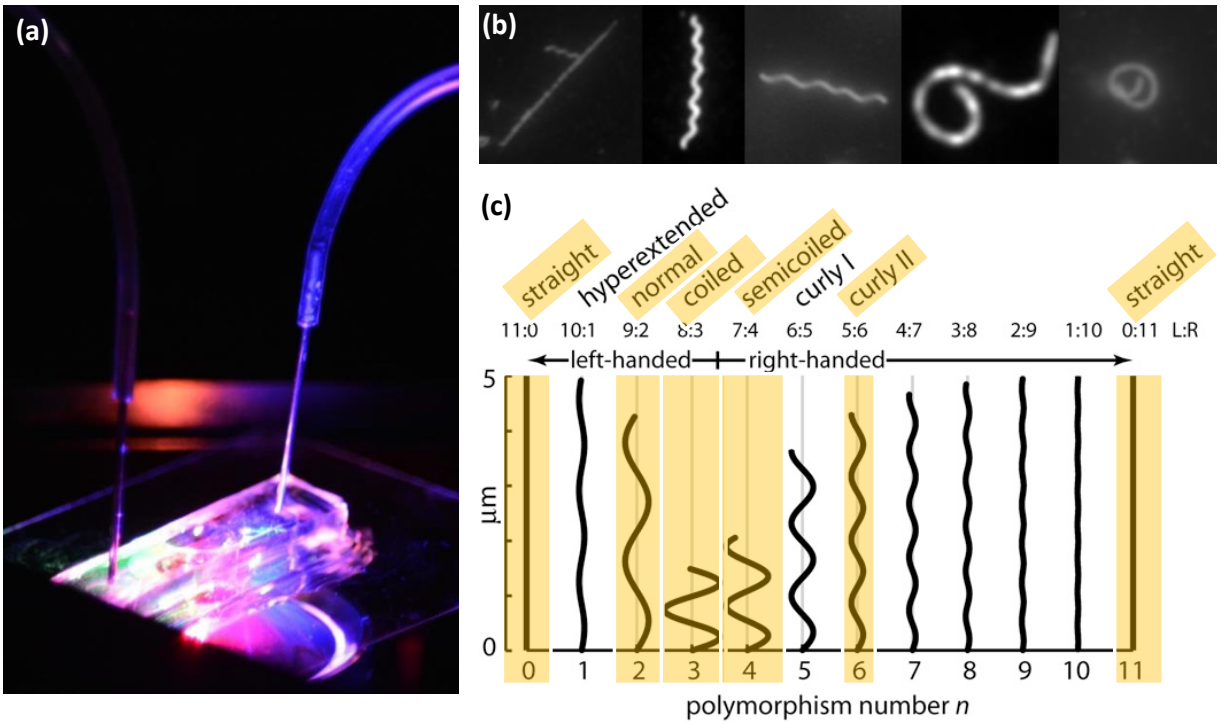

Figure 7: *(a) Microfluidic system used to investigate polymorphic transformations of individual flagella and the flagellar forest (b) Florescence imaging of individual flagella with different polymorphisms (c) Two-dimensional projections of the helical polymorphic forms predicted by the Calladine model of the bacterial flagellum (adapted from [5]). Highlighted are the helical polymorphic forms observed thus far.*

4. EDUCATIONAL IMPACT

In addition to the impact on the proposed DLP/high resolution fluorescence microscopy system on the research programs described in the Section 3, this instrumentation request will also directly support the university-wide vision of multi-scale engineering research and education at Drexel University, especially with two educational initiatives underway: (1) Interdisciplinary Bionanotechnology Graduate Program and (2) an ongoing Nanomanufacturing and Nanometrology Undergraduate Education Program. The PI has led an effort to develop an innovative manufacturing curriculum based on cross-disciplinary and collaborative teaching methodologies to address the impact of nanoscale metrology and manufacturing to the nation and industry, and to introduce science, technology and engineering of discovery-based laboratory metrology and manufacturing to undergraduate students at Drexel University. The PI has developed a set of collaborative lecture and laboratory modules (this educational program is supported by

NSF CCLI program: http://www.nsf.gov/awardsearch/showAward.do?AwardNumber=0941512), in which students get hands on experience with the integrated DLP/high resolution fluorescence microscopy and electromagnetic manipulators through a series of guided laboratory modules.

5. REFERENCES

1. Kim, H., Kim, M.J., *Electric Field Control of Bacteria-Powered Microrobots (BPMs) Using a Static Obstacle Avoidance Algorithm*. Robotics, IEEE Transactions on, 2015. **PP**(99): p. 1-13.
2. Kim, H., Cheang, U.K., Kim, D., Ali, J., Kim, M.J., *Hydrodynamics of a self-actuated bacterial carpet using microscale particle image velocimetry*. Biomicrofluidics, 2015. **9**(2): p. 024121.
3. Cheang, U.K., Kim, M.J., *Self-assembly of robotic micro-and nanoswimmers using magnetic nanoparticles*. Journal of Nanoparticle Research. **17**(3): p. 1-11.
4. Jo, W., U.K. Cheang, Kim, M.J., Development of flagella bio-templated nanomaterials for electronics. Nano Convergence, 2014. **1**(1): p. 1-14.
5. Darnton, N.C., Berg, H.C., *Force-extension measurements on bacterial flagella: triggering polymorphic transformations*. Biophysical journal, 2007. **92**(6): p. 2230-2236.

DURIP Equipment Summary

Nikon Ti-Eclipse

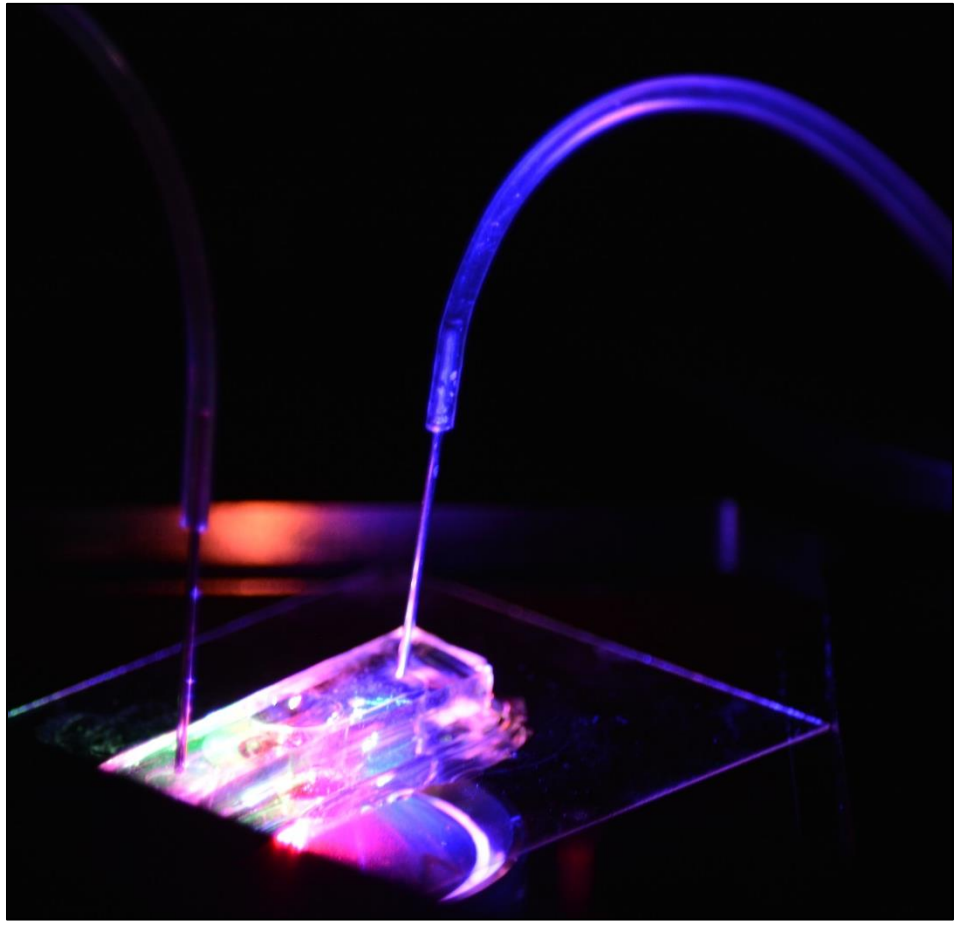

Andor Ixon3

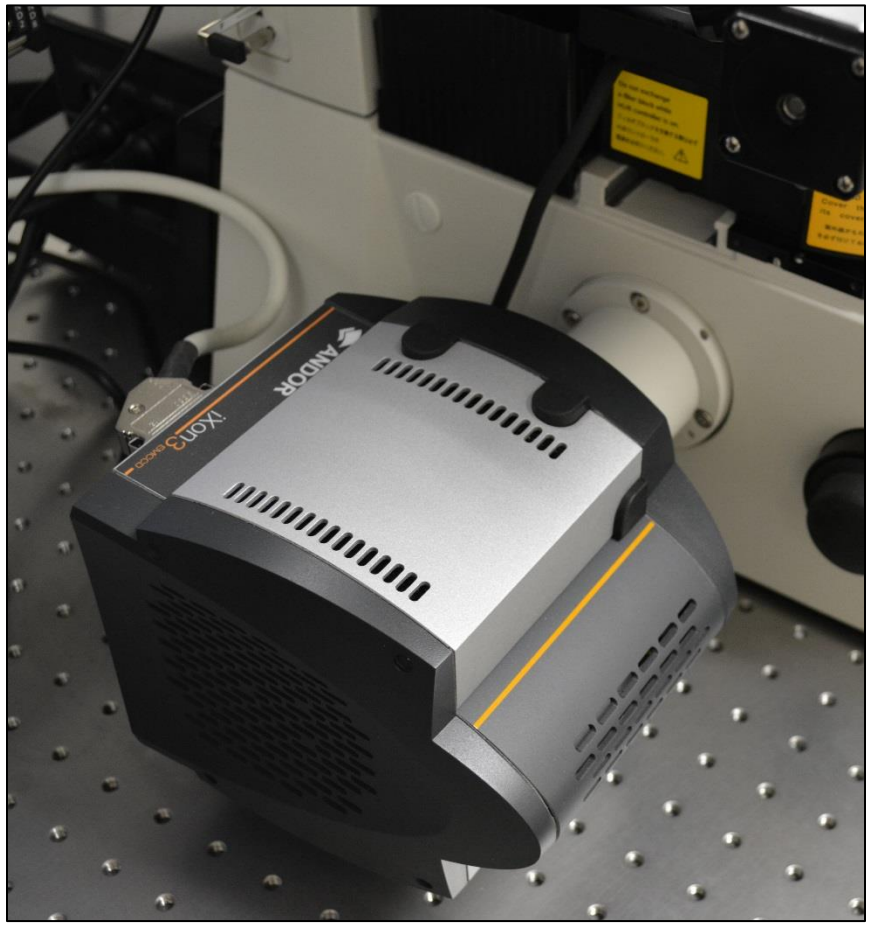

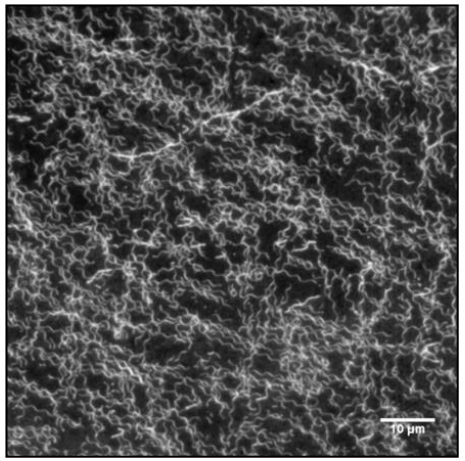

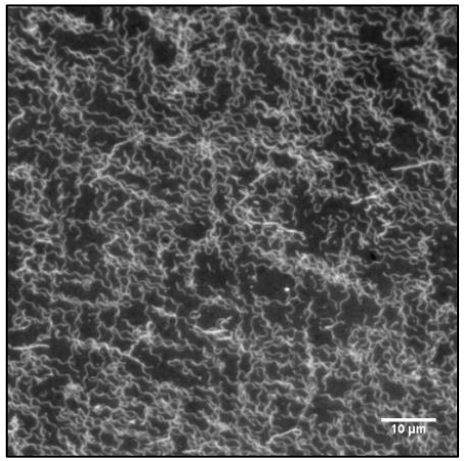

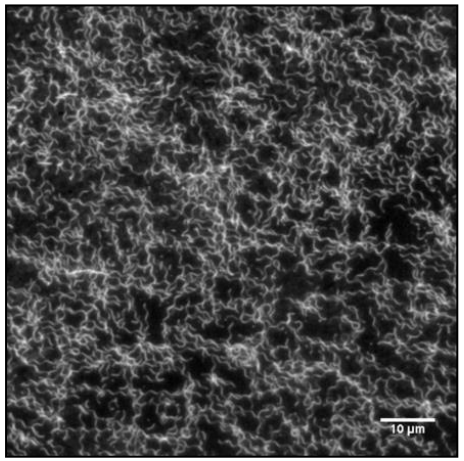

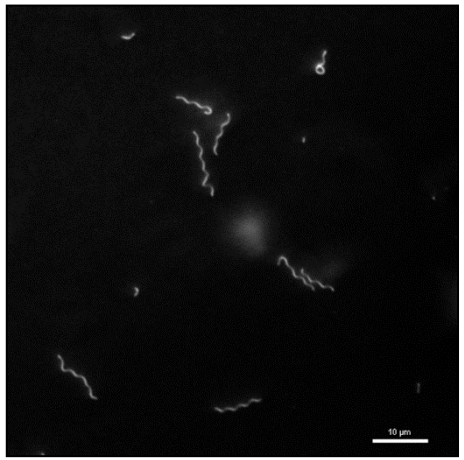

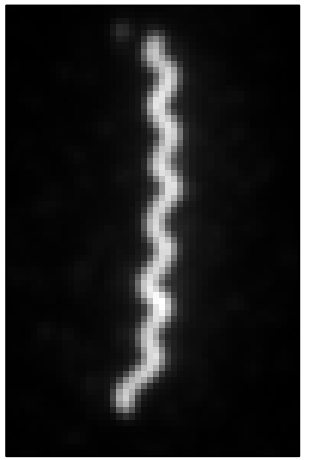

Motorized Turrets and Objectives

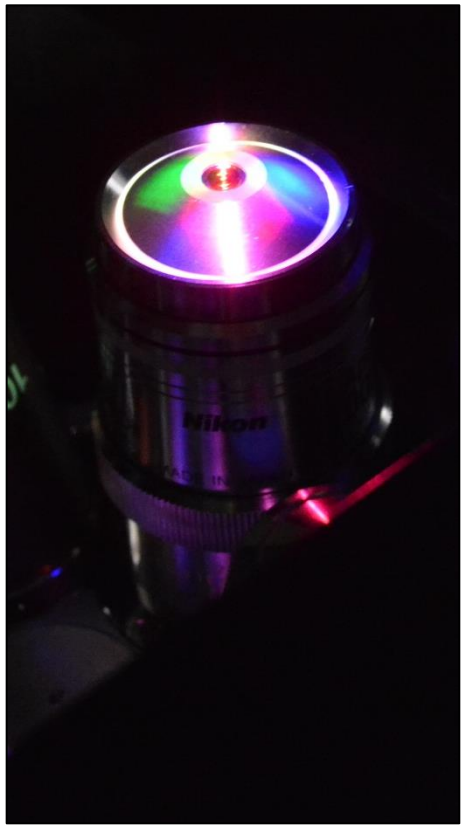

Digital Light Innovations Dli 4120 Discovery System

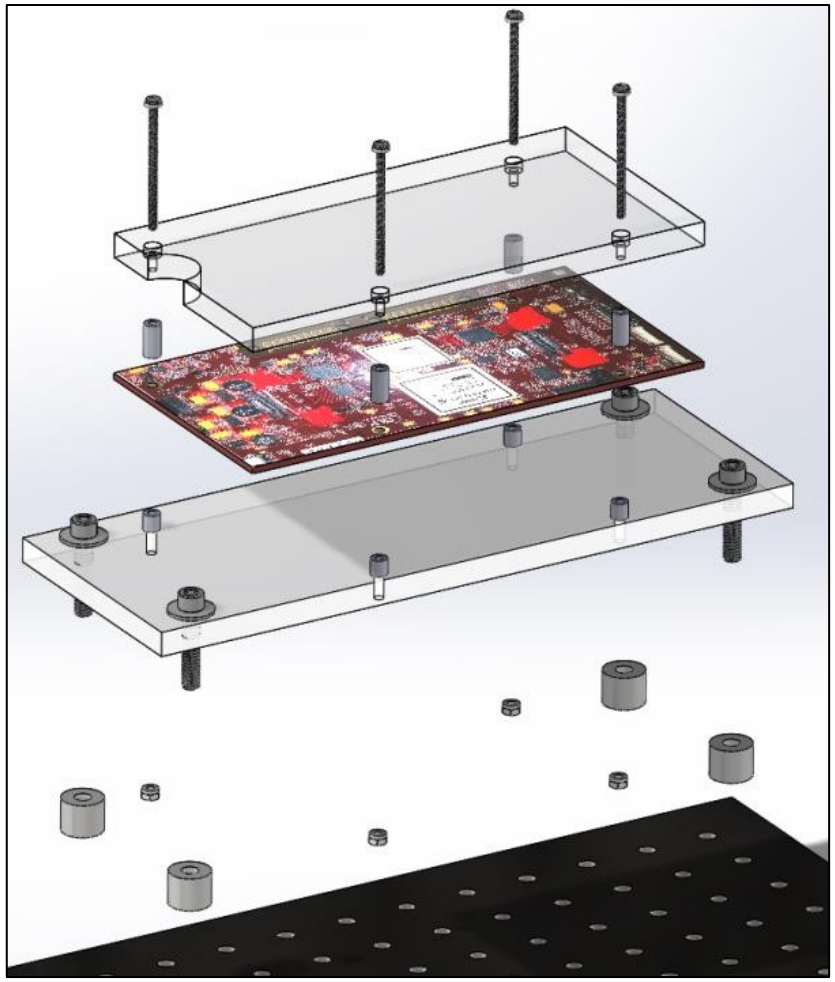

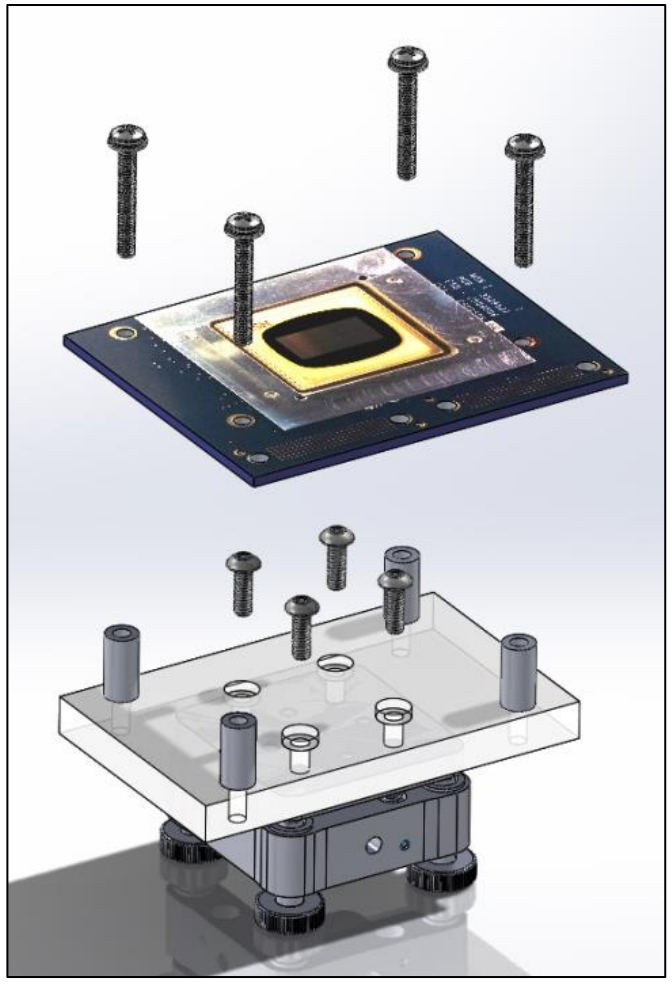

3D Printed Magnetic and Electric Field Controller

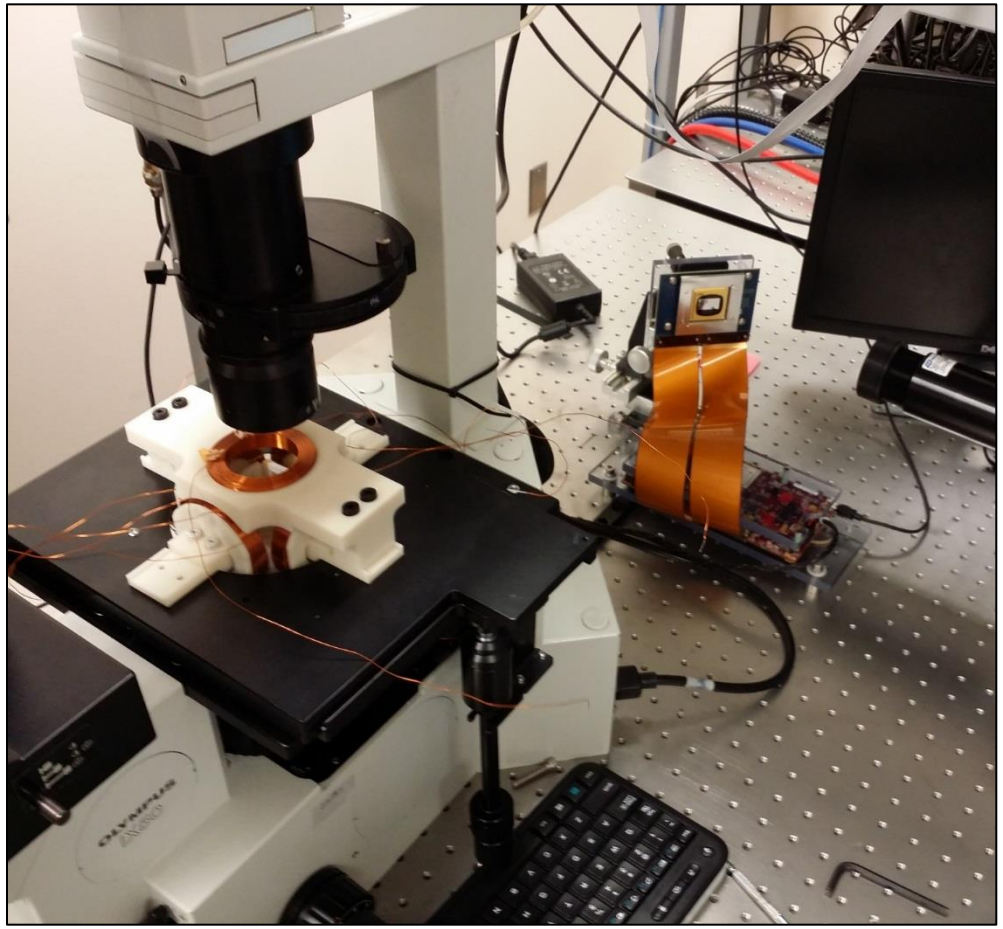

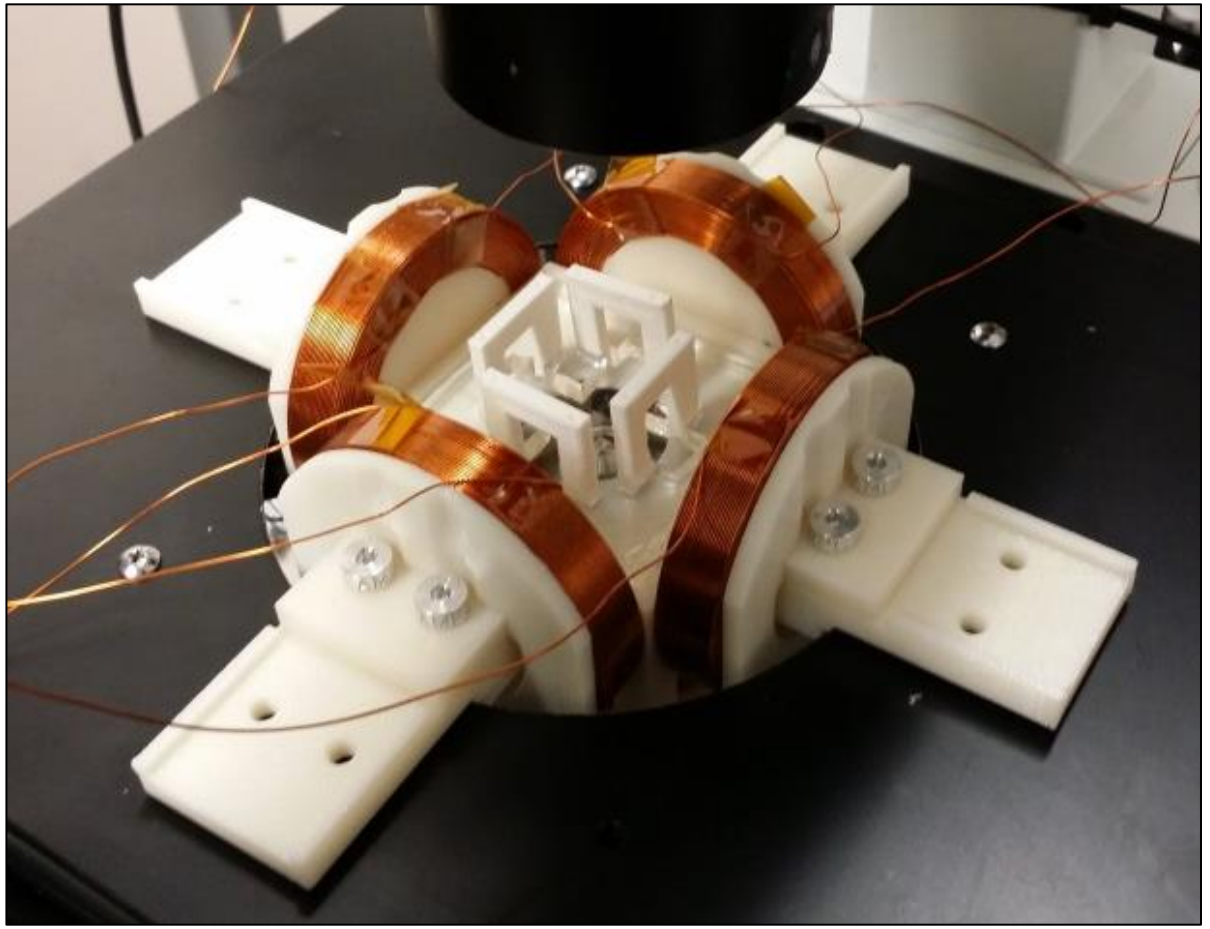

DLP Integration with Microscopes and Laser Sources

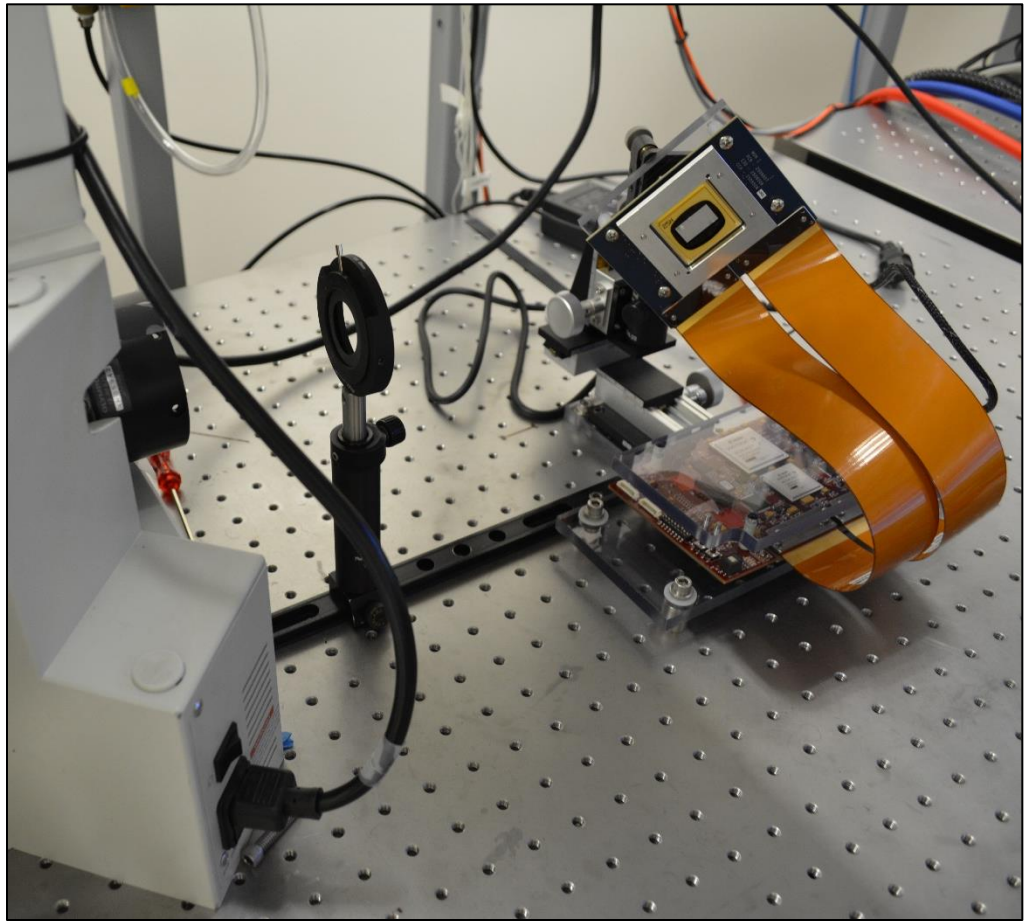

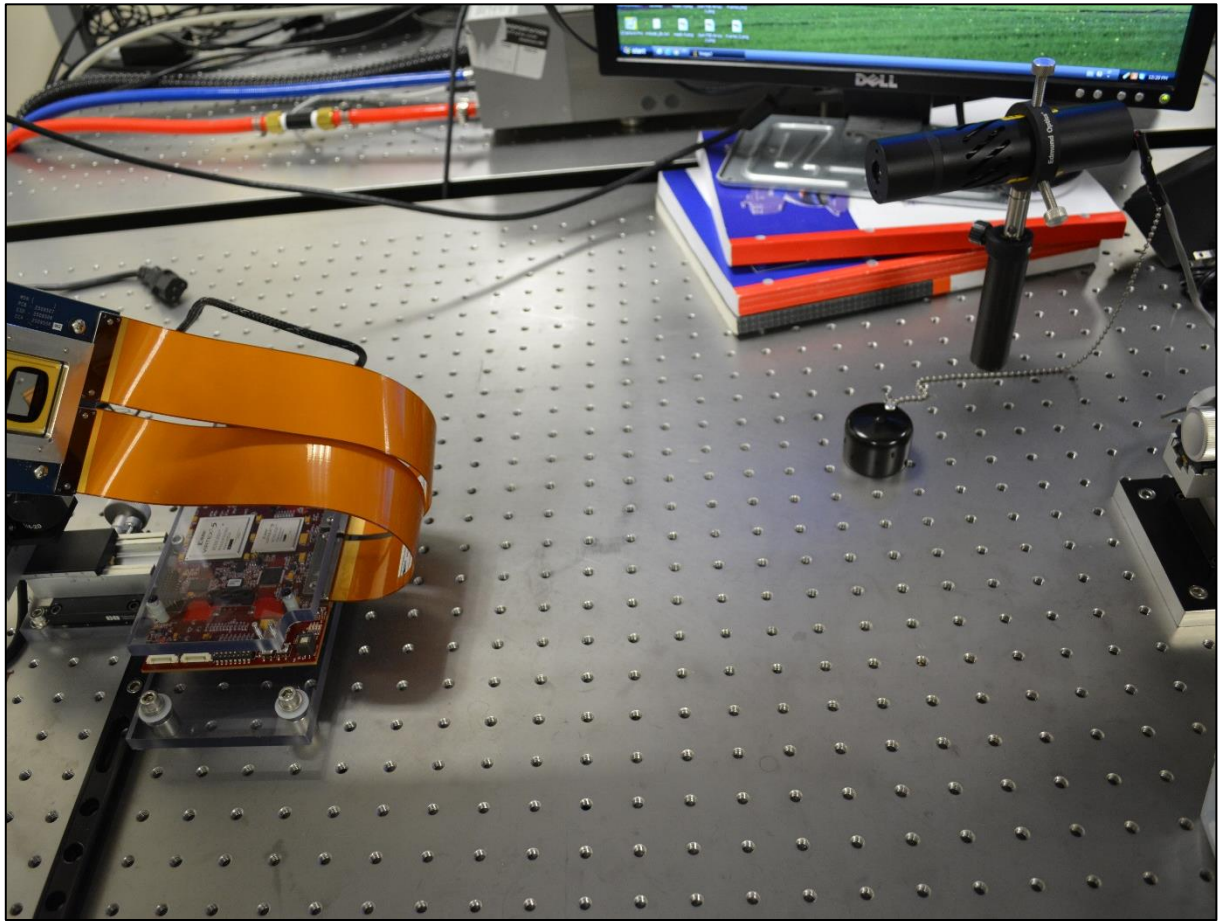

Laser custom mounts

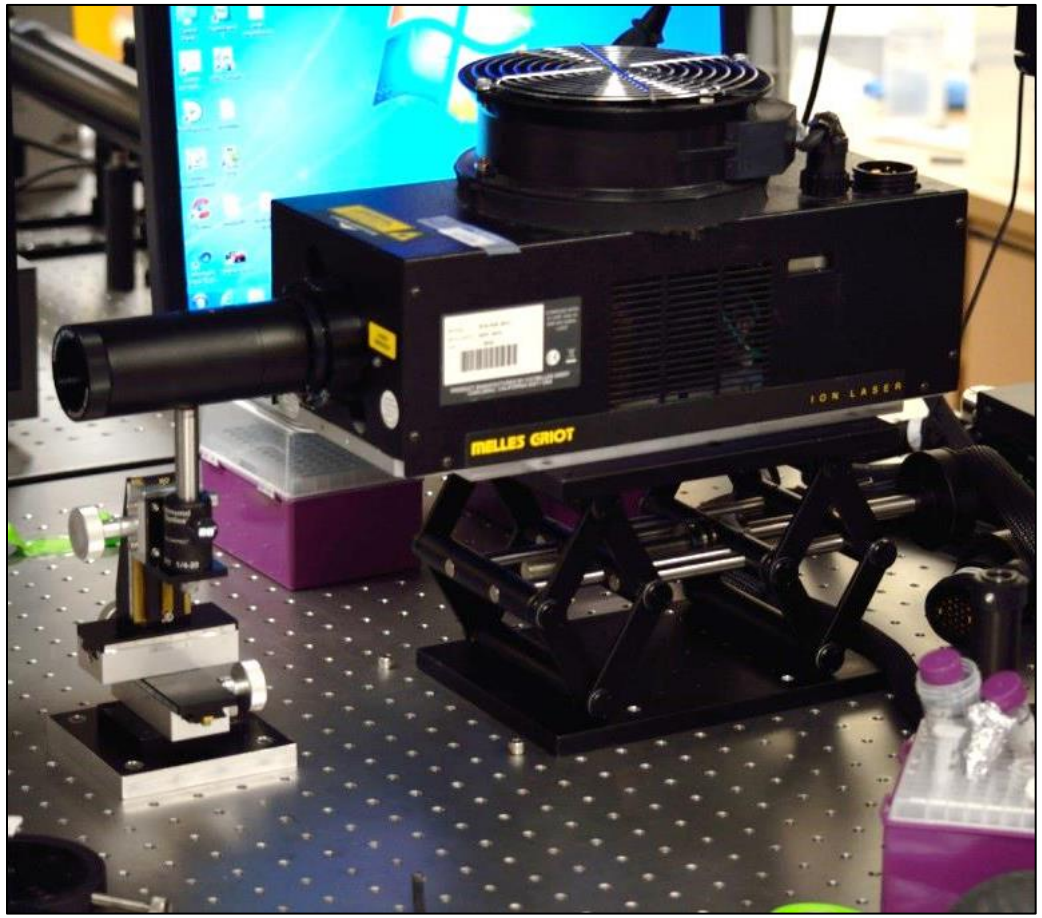

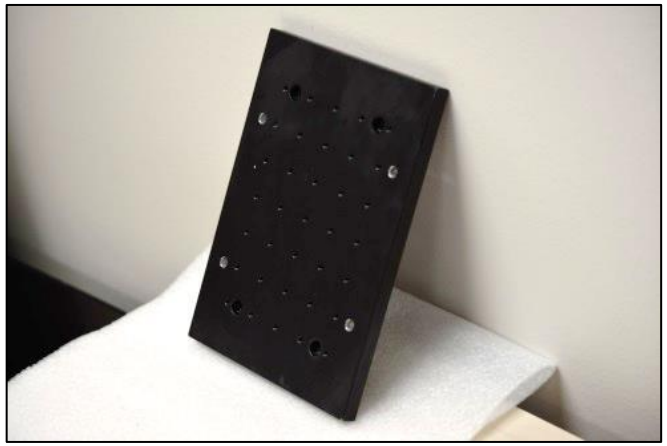

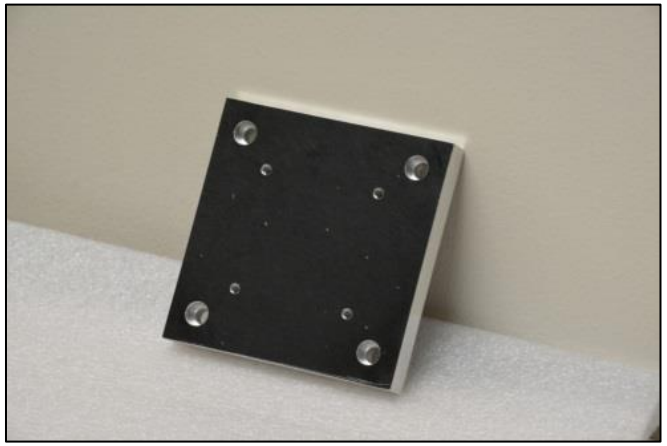

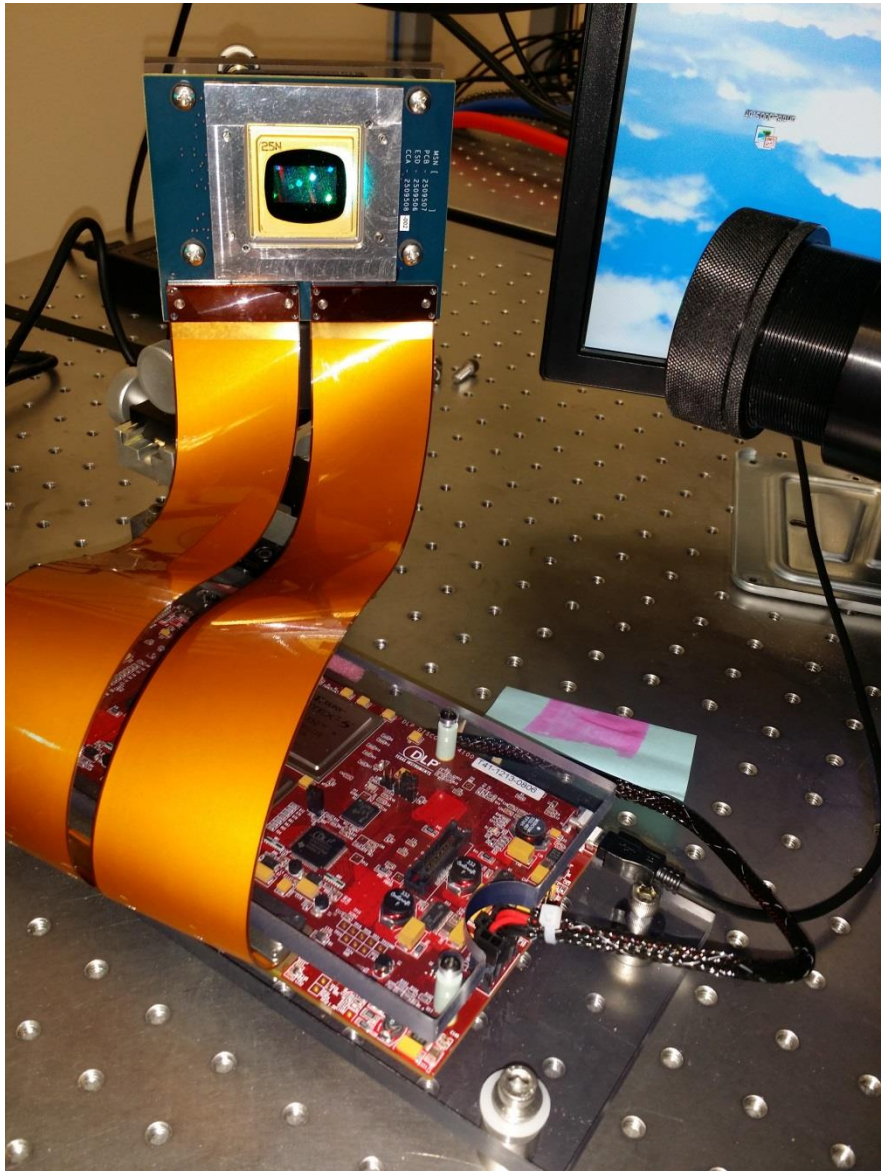

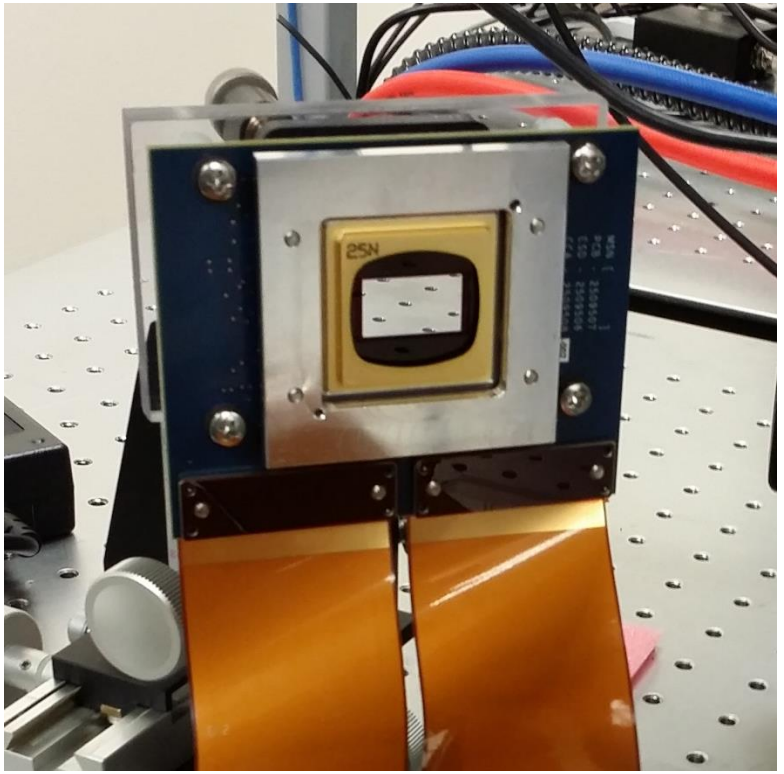

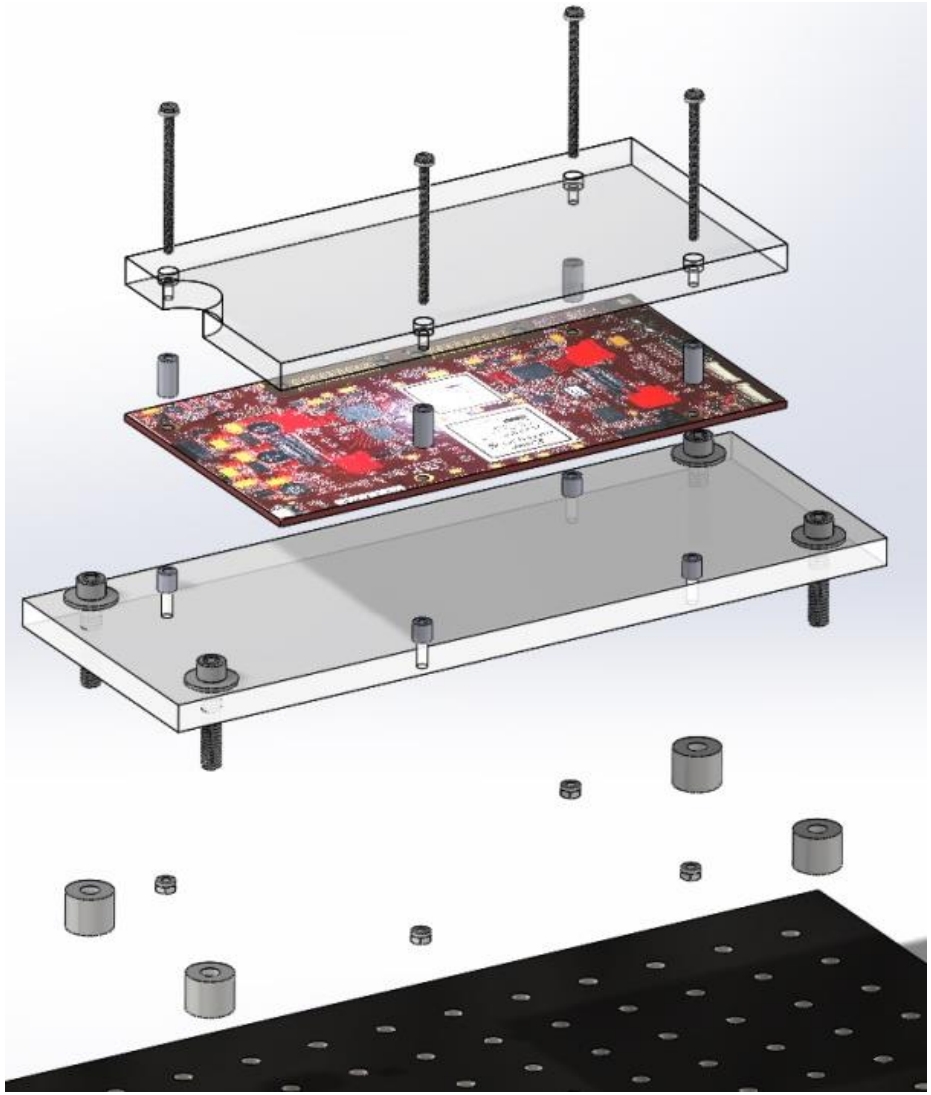

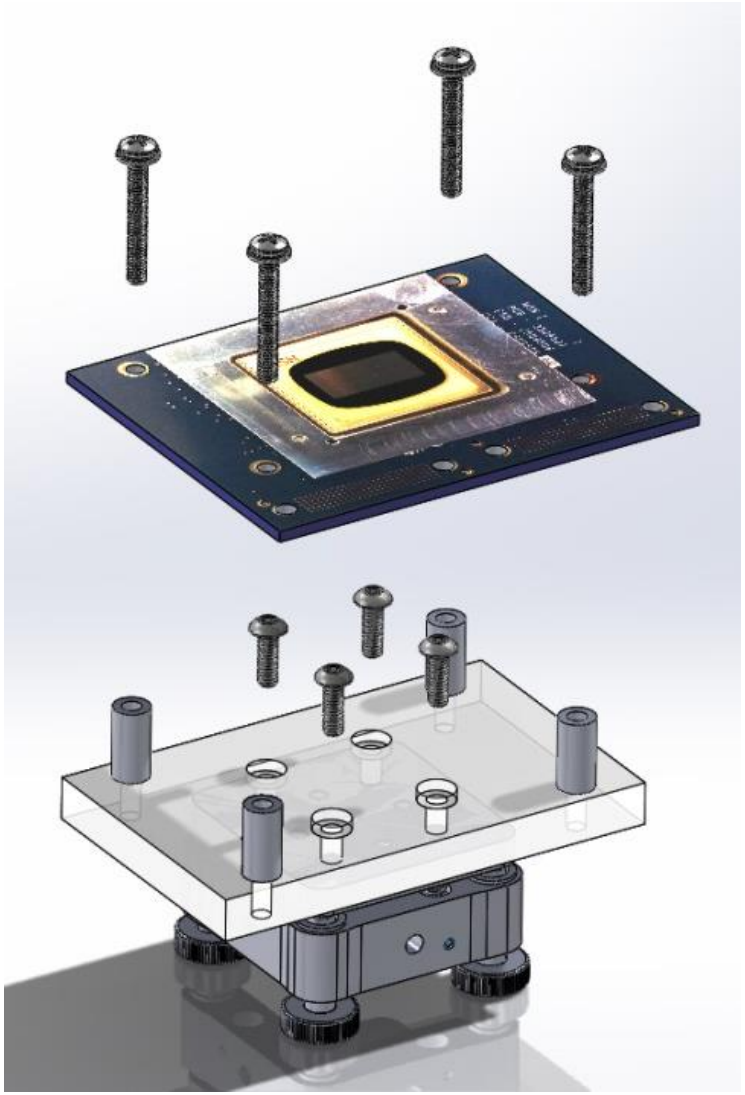

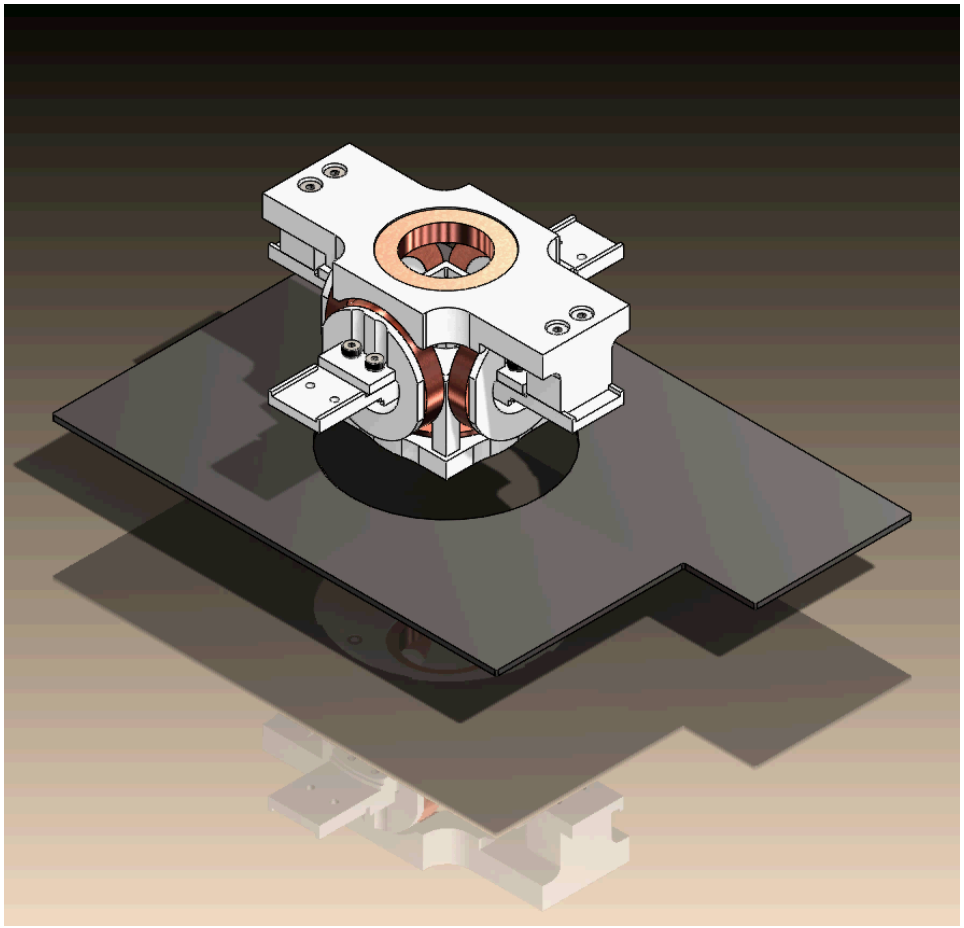

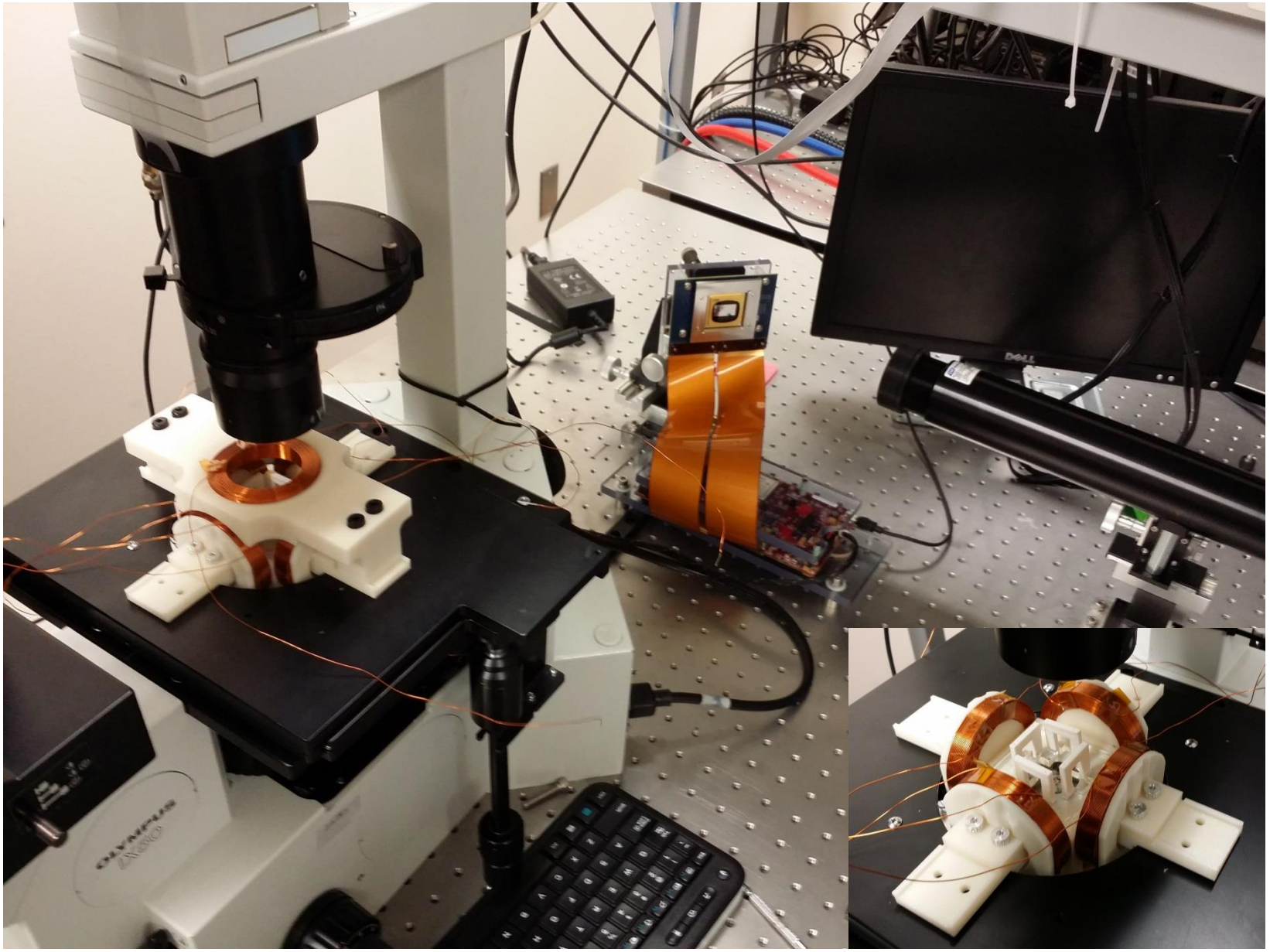
OLYMPUS
DELL